Received: 25 February 2025 | Revised: 4 June 2025 | Accepted: 26 June 2025

DOI: 10.1002/joa3.70140

Journal of Arrhythmia Open Access WILEY

ORIGINAL ARTICLE

Association between aortomitral continuity calcification and conduction disturbances following transcatheter aortic valve implantation with the balloon-expandable Myval valve

Serkan Aslan M.D.[1] | Aysel Türkvatan M.D.[2] | Mehmet Kanyılmaz M.D.[2] | Burçin Yılmaz M.D.[2] | Dilara Pay M.D.[1] | Kadir Sadıkoğlu M.D.[1] | Hande Uysal M.D.[1] | Gökhan Demirci M.D.[1] | Mehmet Altunova M.D.[1] | Serkan Kahraman M.D.[1] | Mehmet Ertürk M.D.[1]

[1]Department of Cardiology, University of Health Sciences Istanbul Mehmet Akif Ersoy Thoracic and Cardiovascular Surgery Training and Research Hospital, Istanbul, Turkey

[2]Department of Radiology, University of Health Sciences Istanbul Mehmet Akif Ersoy Thoracic and Cardiovascular Surgery Training and Research Hospital, Istanbul, Turkey

Correspondence
Serkan Aslan, Istanbul Mehmet Akif Ersoy Hastanesi, Istasyon Mahallesi, Turgut Ozal Bulvarı, No. 11, Kucukcekmece/Istanbul 34303, Turkey.
Email: drserkanaslan@gmail.com

Abstract

Background: Given the anatomical proximity of the cardiac conduction system, aortomitral continuity calcification (AMCC) may contribute to conduction disturbances (CD) during transcatheter aortic valve implantation (TAVI) due to radial force on the AMCC. This study aimed to investigate the impact of AMCC on new-onset CD in patients undergoing TAVI with the balloon-expandable Myval valve.

Methods: This retrospective study included 160 patients who underwent TAVI. AMCC was assessed using Agatston and calcium volume scores from preprocedural computed tomography (CT). Multivariable logistic regression was used to identify independent predictors of CD.

Results: High-grade atrioventricular block (HAVB) occurred in 13.1% of patients, and 17.5% required permanent pacemaker implantation (PPM). Patients with HAVB and PPM exhibited a higher prevalence of AMCC and significantly higher AMCC scores. An AMCC score >180 was an independent predictor of HAVB (OR, 5.58; 95% CI, 1.43–21.70; $p = .013$) and PPM (OR, 5.39; 95% CI, 1.75–16.55; $p = .002$). When classified by AMCC proximity type, right fibrous trigone (RFT)-dominant calcification was a strong independent predictor of HAVB (OR, 9.22; 95% CI, 1.63–51.99; $p = .012$) and PPM (OR, 7.62; 95% CI, 1.91–30.38; $p = .004$). Prolonged QRS duration, greater implantation depth, and shorter membranous septum length were also independent predictors.

Conclusion: AMCC is a strong independent predictor of HAVB and PPM following TAVI, particularly with scores >180 or when AMCC is anatomically close to the RFT. Preprocedural CT-based assessment of AMCC burden and proximity may improve risk stratification and procedural planning.

KEYWORDS
aortomitral continuity, computed tomography, conduction disturbance, permanent pacemaker implantation, transcatheter aortic valve implantation

1 | INTRODUCTION

Transcatheter aortic valve implantation (TAVI) has become a widely utilized treatment option for patients with severe symptomatic aortic stenosis who are at an intermediate to high operative risk for surgery.[1,2] While TAVI has proven to be a life-saving procedure, improving hemodynamics and symptoms in these patients, it is not without complications. One of the most common and clinically significant postprocedural complications is the development of conduction disturbances (CD), which can manifest as high-degree atrioventricular block (HAVB) requiring permanent pacemaker (PPM) implantation.[3,4]

The aortomitral continuity (AMC) is located between the anteromedial aspects of the mitral annulus and the aortic valve, and has a direct anatomical relationship with the aortic valve apparatus. Moreover, the AMC is linked to the right fibrous trigone (RFT) via the membranous septum (MS).[5] Aortomitral continuity calcification (AMCC) may interfere with the atrioventricular (AV) conduction axis, increasing the risk of arrhythmias and CD including HAVB following the procedure. This phenomenon can be attributed to the considerable radial forces exerted by the expanding prosthesis on the AV node and its bundle fibers, situated within the MS and the central fibrous body, which are in close proximity to the aortic annulus.[6,7] However, the exact mechanisms and clinical significance of this relationship remain incompletely understood. Only a limited number of studies have investigated the impact of AMC on its alterations following TAVI with early generation transcatheter heart valve (THV) devices.[8–10] Myval (Meril Life Sciences Private Ltd., Gujarat, India) is a next-generation balloon-expandable THV with novel features to improve safety and efficacy, but its interaction with left ventricular outflow tract (LVOT) anatomy, specifically AMCC, has not been examined to date.

The present study aimed to investigate whether imaging of the AMCC by computed tomography (CT) can be used to identify patient-specific anatomic risk of HAVB and PPM before TAVI with balloon-expandable Myval valve.

2 | METHODS

2.1 | Study population and design

We retrospectively reviewed the CT scans of 171 consecutive patients who underwent TAVI at our institution between February 2021 and September 2024. All patients had severe symptomatic aortic stenosis with an initial aortic valve area (AVA) of ≤1.0 cm^2 and an indexed AVA (AVA/body surface area) of <0.6 cm^2/m^2. Exclusion criteria included previous PPM implantation ($n=4$), the presence of valve replacement or repair: aortic ($n=2$) and/or mitral ($n=3$), patients without preprocedural noncontrast CT ($n=1$), and intraprocedural death ($n=1$). The final data analysis of the study included 160 patients. We report the 30-day outcomes of all subjects enrolled in this study, which focused on the relationship between CD and AMCC in patients undergoing TAVI with the Myval THV. The primary endpoint was defined as the occurrence of HAVB or the need for PPM implantation for new-onset CD. Baseline clinical, electrocardiographic, procedural, and postprocedural characteristics were obtained from our institutional database. The study was conducted according to the Helsinki Declaration and was approved by the hospital's Institutional Review Board.

2.2 | CT acquisition and image analysis

2.2.1 | CT acquisition

All examinations were performed on a 320-detector-row CT scanner (Aquilion ONE, Toshiba Medical Systems, Otawara, Japan) with a gantry rotation time of 350 ms. As previously described, the TAVI protocol includes a prospective electrocardiogram (ECG)-gated noncontrast scan, a prospective ECG-gated (20%–70% of R–R interval) axial one-beat acquisition of the aortic root and heart, and a non-ECG-gated thoracic-abdominal-pelvic CT angiography for evaluation of peripheral vascular access with a single bolus of contrast.[7] Imaging data were acquired during the intravenous injection of 60–100 mL of contrast (Iohexol, Omnipaque 350 mg/mL; GE Healthcare, Milwaukee, WI) at a flow rate of 5.0 mL/s, followed by a 40–60 mL saline chaser at the same flow rate. The scan delay was determined using a bolus tracking technique with the region of interest placed in the descending aorta and the trigger threshold set at 180 Hounsfield units (HU). Tube voltage and current were adjusted for body mass index (BMI). The tube voltage was set to 100 kV (BMI ≤30 kg/m^2) or 120 kV (BMI >30 kg/m^2), and the tube current was set to 320–480 mA. CT images were reconstructed to a thickness of 0.5 mm using an iterative reconstruction algorithm.

2.2.2 | CT image analysis

CT images were reviewed independently by two experienced radiologists who were blinded to the patients' clinical and procedural data. A dedicated postprocessing workstation (Aquarius iNtuition version 4.4.11, Terarecon Inc., Foster City, CA) was used to generate multiplanar reconstructions for precise localization and quantification of calcifications. Quantitative assessment of aortic valve calcification (AVC), mitral annular calcification (MAC), and AMCC was performed

on noncontrast ECG-gated CT images using both the Agatston score and calcium volume score. CT attenuation values >130 HU were used to define calcification. The Agatston score is a cumulative value of all calcified lesions based on both total area and maximum density of calcification. CT attenuation greater than 130 HU is used to identify calcium in contiguous 1 mm^2 voxels, which are then counted as discrete calcified lesions.[11] To calculate the calcium volume score, the volume of each voxel, as determined by area and slice thickness, is multiplied by the number of voxels showing calcification. This is achieved by using a threshold of >130 HU for attenuation of the HU. As previously stated, the Agatston score is a composite of area multiplied by a density factor, whereas the volume score is the volume of calcium, independent of calcium density.

AMCC was defined as the presence of calcification between the anteromedial aspects of the mitral annulus and the aortic valve, the posterior aspect of the LVOT (Figure 1). The contrast-enhanced CT images were used to identify the AMC region in the LVOT view. The AMC region was defined as above the mitral annulus plane and below the aortic annulus plane. LVOT calcification was defined as the presence of calcification in the anterior aspect of the LVOT. AMCC lesions showing continuity with AVC or MAC were isolated from AVC or MAC by circling the region of interest. To enable anatomical stratification, the spatial distribution of AMCC was categorized based on its proximity to the fibrous trigones: RFT-dominant (closer to the RFT), left fibrous trigone (LFT)-dominant (closer to the LFT), or bilateral (involving both trigonal regions). This proximity-based classification was independently assessed by both radiologists, with discordances resolved by consensus. MAC was defined as the presence of calcification at the base of the mitral leaflets at the level of the mitral annulus.

The eccentricity of the aortic annulus was calculated using the following formula: It is calculated by subtracting the minimum diameter from the maximum diameter. MS length was determined by measuring the distance between the plane of the aortic annulus and the crest of the muscular interventricular septum in the coronal view.[12]

2.3 | Technical aspects of TAVI

All patients underwent TAVI after a comprehensive evaluation and discussion by the cardiac team. All TAVI procedures were performed utilizing a balloon-expandable Myval THV, which is available in a range of sizes (traditional, 20, 23, 26, and 29 mm; intermediate, 21.5, 24.5, and 27.5 mm; and extra-large, 30.5 and 32 mm) via a transfemoral approach. The THV size was selected based on CT measurements of the aortic valve annulus according to the manufacturer's recommendations. The decision to perform predilatation and/or postdilatation was at the discretion of the operator. In the majority of cases, predilatation was performed in cases where more than mild calcifications were present to ensure full valve expansion. In cases of residual moderate to severe paravalvular leak and/or valve underexpansion, postdilatation was considered. As previously described, implantation depth (ID) was measured angiographically and defined as the distance from the deepest part of the noncoronary cusp to the distal end of the prosthetic valve.[13]

2.4 | Electrocardiography

A 12-lead surface ECG was recorded from each patient at baseline (within 24 hours prior to procedure) and was obtained as a daily 12-lead ECG during the time of hospitalization.[14] All patients underwent cardiac rhythm monitoring for a minimum of 24 hours following the procedure. All ECGs were reviewed for pre- and postoperative conduction abnormalities such as left bundle branch block (LBBB), right bundle branch block (RBBB), prolonged PR interval, new-onset atrial fibrillation, and HAVB, as defined by the American Heart

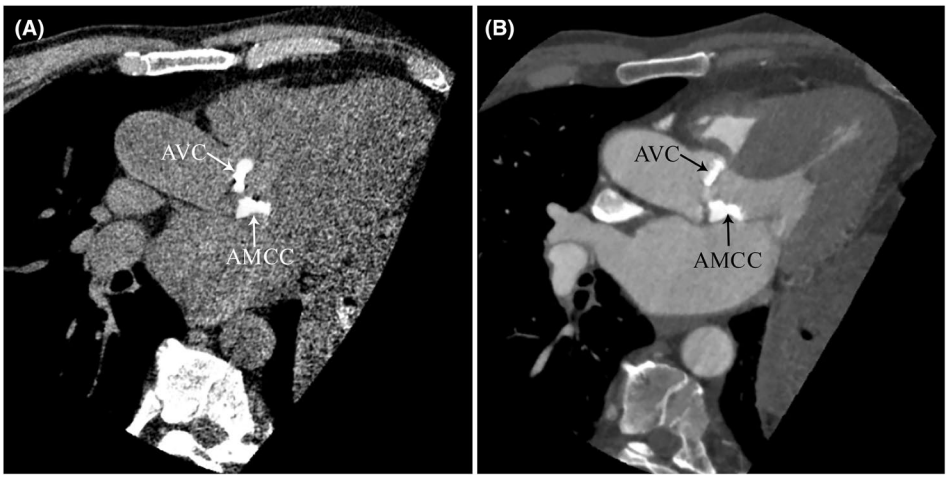

FIGURE 1 Example of severe aortomitral continuity calcification (AMCC) on computed tomography (CT). A 79-year-old male patient with conduction disturbance. Noncontrast (A) and contrast-enhanced (B) CT images of the left ventricular outflow tract show aortic valve calcification (AVC) and AMCC. The AMCC score was calculated as 268 using the Agatston score method and 234 mm^3 using the volume score method.

Association/American College of Cardiology recommendations for ECG standardization and interpretation.[15] HAVB was defined as the presence of either Mobitz type II second-degree AV block or third-degree AV block. Patients with persistent HAVB at 24–48 h post-TAVI underwent PPM implantation in accordance with current European guidelines.[16] The final decision for PPM is at the discretion of the electrophysiologist, considering in-hospital ECG evolution and clinical data.

2.5 | Statistical analysis

Analyses were performed using the Statistical Package for the Social Sciences (SPSS) version 24 software package (SPSS Inc., Chicago, Illinois, USA). Continuous variables were tested for normality of distribution using both graphical (histograms) and numerical methods (Kolmogorov–Smirnov and Shapiro–Wilk tests). Results were presented as mean ± SD or median and interquartile range. These variables were compared using a two-tailed Student's *t*-test or Mann–Whitney test, as appropriate. Categorical data were presented as numbers and percentages and compared using the Pearson chi-squared test or Fisher's exact test. For statistical analysis, AMCC burden was stratified into three categories based on its distribution: score = 0 (median score), 1–180 (interquartile range), and >180 (above 75th percentile). The first category consisted of scores equal to zero, which represented the median score. The next category included scores between one and 180, representing a value between the 50th and 75th percentiles. The final category included scores greater than 180, indicating a value greater than the 75th percentile. These thresholds were used in multivariable regression models. The anatomical AMCC proximity types (RFT-dominant, LFT-dominant, and bilateral) were analyzed separately as categorical predictors in a dedicated multivariable model. The multivariable models were constructed by selecting variables that met the entry criterion of $p < .1$ in a univariable CD analysis. Results were interpreted in terms of confidence intervals (CI) for the odds ratio (OR). A two-tailed *p*-value of less than .05 was considered statistically significant.

3 | RESULTS

3.1 | Baseline characteristics

Of the 160 included patients, HAVB developed in 21 (13.1%) after TAVI. The majority of HAVBs occurred immediately after valve implantation (18/21). HAVB occurred in the early postoperative period in three patients (2 within 24 h and 1 within 24–48 h after surgery), all of whom developed in the intensive care unit (ICU). Of the three patients, two had pre-existing RBBB, while the remaining patient developed complete LBBB with a prolonged PR interval following the procedure. Twenty-eight patients (17.5%) received PPM implantation. The median time to PPM implantation was 6 days (interquartile range, 3–8 days). The indications for PPM included third-degree AV block ($n = 17$), second-degree AV block Mobitz type II ($n = 4$), complete LBBB with a prolonged PR interval ($n = 4$), alternating bundle branch block ($n = 1$), symptomatic sick sinus syndrome with documented bradycardia ($n = 1$), and atrial fibrillation with low ventricular response resulting in hemodynamic instability ($n = 1$). The baseline characteristics of the study population are summarized in Table 1. The mean age of the patients was 79.3 ± 7.0 years, with 73 individuals (45.6%) being male. The most prevalent comorbidities were coronary artery disease (83.1%), hypertension (73.8%), and diabetes mellitus (40.6%). The primary baseline characteristics exhibited no notable differences between the two subgroups except for QRS duration and RBBB. Patients with QRS prolongation were more likely to have HAVB (108.8 ± 24.4 vs. 93.7 ± 15.5, $p < .001$) and PPM (105.2 ± 22.3 vs. 93.7 ± 15.8, $p = .001$). RBBB was significantly associated with both HAVB ($p = .017$) and PPM implantation ($p = .038$).

3.2 | CT Characteristics

Table 2 shows the CT characteristics. 45.0% of patients exhibited AMCC. Patients with HAVB (71.4% vs. 41.0%; $p = .009$) or PPM (71.4% vs. 39.4%; $p = .002$) had a significantly higher prevalence and burden of AMCC. Median AMCC Agatston score was markedly elevated in these patients (182 vs. 0, $p = .038$ for HAVB; 172 vs. 0, $p = .009$ for PPM). Stratification into three AMCC categories (score 0, 1–180, >180) revealed a stepwise increase in HAVB and PPM incidence with increasing AMCC severity ($p = .006$ and $p = .002$, respectively) (Figure 2). In summary, patients in the highest category (AMCC >180) exhibited a significantly higher incidence of HAVB (27.5% vs. 6.8%, $p = .001$) and PPM implantation (35.0% versus 9.1%, $p < .001$) compared to those in the lowest category.

A significant association was observed between AMCC proximity type and new-onset CD. Patients with RFT-dominant AMCC had the highest incidence of HAVB (26.9% for RFT-dominant; 14.3% for LFT-dominant; 18.8% for bilateral, $p = .040$) and PPM (34.6% for RFT-dominant; 14.3% for LFT-dominant; 28.1% for bilateral, $p = .007$), followed by bilateral involvement (Table 2). MAC and AVC did not differ significantly, but MS length was shorter in patients with HAVB (5.4 ± 0.9 mm vs. 6.3 ± 1.0 mm; $p < .001$) and PPM (5.6 ± 1.1 mm vs. 6.4 ± 1.0 mm; $p = .001$).

3.3 | Procedural Characteristics

Procedural characteristics are summarized in Table 3. Patients with HAVB exhibited a larger valve size compared to patients without HAVB ($p = .038$). In contrast, patients in the PPM group had a larger valve size, although this difference was not statistically significant ($p = .074$). The ID was significantly higher for patients

TABLE 1 Baseline patient characteristics.

	All patients (*N* = 160)	High-degree AV block			PPM implantation		
		No (*N* = 139)	Yes (*N* = 21)	*p*-Value	No (*N* = 132)	Yes (*N* = 28)	*p*-Value
Clinical variables							
Age (years)	79.3 ± 7.0	79.1 ± 7.3	81.1 ± 4.3	.228	79.2 ± 6.7	79.8 ± 8.1	.665
Sex (male)	73 (45.6)	62 (44.6)	11 (52.4)	.505	58 (43.9)	15 (53.6)	.353
Hypertension	118 (73.8)	101 (72.7)	17 (81.0)	.421	96 (72.7)	22 (78.6)	.523
Diabetes mellitus	65 (40.6)	57 (41.0)	8 (38.1)	.800	55 (41.7)	10 (35.7)	.560
Coronary artery disease	133 (83.1)	115 (82.7)	18 (85.7)	1.0	109 (82.6)	24 (85.7)	.789
Previous CABG	26 (16.3)	25 (18.0)	1 (4.8)	.203	23 (17.4)	3 (10.7)	.573
Peripheral artery disease	11 (6.9)	10 (7.2)	1 (4.8)	1.0	10 (7.6)	1 (3.6)	.691
Chronic lung disease	29 (18.1)	25 (18.0)	4 (19.0)	1.0	25 (18.9)	4 (14.3)	.562
Chronic kidney disease	33 (20.6)	32 (23.0)	1 (4.8)	.079	30 (22.7)	3 (10.7)	.154
Previous Stroke/TIA	8 (5.0)	8 (5.8)	0 (0.0)	.598	8 (6.1)	0 (0.0)	.352
Paroxysmal or persistent atrial fibrillation	42 (26.3)	38 (27.3)	4 (19.0)	.421	37 (28.0)	5 (17.9)	.266
STS score: mortality (%)	5.0 (3.3–6.0)	4.9 (3.3–6.0)	5.0 (3.3–5.9)	.997	5 (3.6–6.0)	4.1 (3.0–5.6)	.371
Preprocedural echocardiography							
LVEF (%)	51.9 ± 12.5	51.3 ± 13.0	55.4 ± 7.9	.170	51.4 ± 13.1	54.2 ± 9.3	.288
Aortic valve area (cm^2)	0.73 (0.63–0.80)	0.72 (0.63–0.81)	0.77 (0.65–0.80)	.821	0.73 (0.63–0.81)	0.68 (0.61–0.80)	.599
Maximum aortic gradient (mmHg)	76.4 ± 23.2	76.1 ± 23.3	78.3 ± 22.8	.691	75.7 ± 23.4	79.5 ± 22.4	.445
Mean aortic gradient (mmHg)	46.8 ± 14.4	46.5 ± 14.3	49.2 ± 15.3	.425	46.2 ± 14.4	49.7 ± 14.5	.244
Aortic peak systolic velocity (m/s)	4.33 ± 0.70	4.32 ± 0.70	4.40 ± 0.68	.623	4.31 ± 0.71	4.43 ± 0.64	.405
Baseline electrocardiogram							
Sinus rhythm	124 (77.5)	107 (77.0)	17 (81.0)	.787	101 (76.5)	23 (82.1)	.517
Atrial fibrillation	36 (22.5)	32 (23.0)	4 (19.0)	.787	31 (23.5)	5 (17.9)	.517
Heart rate (beats/min)	74.5 ± 14.9	75.0 ± 14.7	71.1 ± 15.8	.275	74.8 ± 15.0	72.9 ± 14.8	.546
PR interval (ms)	172.9 ± 39.8	172.3 ± 34.9	176.8 ± 62.8	.653	171.6 ± 35.1	178.3 ± 56.2	.464
QRS duration (ms)	95.7 ± 17.6	93.7 ± 15.5	108.8 ± 24.4	<.001	93.7 ± 15.8	105.2 ± 22.3	.001
RBBB	5 (3.1)	2 (1.4)	3 (14.3)	.017	2 (1.5)	3 (10.7)	.038
LBBB	8 (5.0)	5 (3.6)	3 (14.3)	.071	5 (3.8)	3 (10.7)	.146

Note: Values represent mean ± SD, *n* (%), or median (interquartile range).

Abbreviations: AV, atrioventricular; CABG, coronary artery bypass grafting; LBBB, left bundle branch block; LVEF, left ventricular ejection fraction; PPM, permanent pacemaker; RBBB, right bundle branch block; STS, Society of Thoracic Surgeons; TIA, transient ischemic attack.

with new-onset HAVB (8.0 ± 1.4 mm vs. 6.4 ± 2.0 mm, respectively; $p = .002$) and PPM (7.8 ± 1.5 mm vs. 6.4 ± 2.0 mm, respectively; $p = .001$) when compared to those without. Predilatation was associated with increased HAVB risk ($p = .046$). A trend toward a higher incidence of PPM was observed in patients with predilatation, although this did not reach statistical significance ($p = .053$). Longer ICU stays and hospitalization durations were observed in patients with HAVB (4 vs. 2; $p = .037$) and PPM (4 vs. 2; $p = .021$). The prolonged ICU stay in these groups was due to continuous electrocardiographic monitoring and complete bed rest until a PPM was implanted.

3.4 | Predictors of HAVB and PPM

Tables 4 and 5 present the logistic regression analyses for HAVB and PPM, respectively. Univariable predictors for both outcomes included prolonged QRS duration, shorter MS length, greater ID, and the presence and extent of AMCC. In multivariable models, AMCC emerged as a consistent independent predictor, regardless of its classification as a categorical variable (>180 score), binary presence/absence, or anatomical proximity. Specifically, patients with AMCC scores >180 had a 5.58-fold increased risk of HAVB (OR, 5.58; 95% CI, 1.43–21.70; $p = .013$) and a 5.39-fold increased risk of

TABLE 2 Computed tomography characteristics.

	All patients (*N* = 160)	High-degree AV block		*p*-Value	PPM implantation		*p*-Value
		No (*N* = 139)	Yes (*N* = 21)		No (*N* = 132)	Yes (*N* = 28)	
Annulus eccentricity (%)	0.24 (0.20–0.28)	0.25 (0.20–0.28)	0.24 (0.20–0.29)	.604	0.25 (0.20–0.27)	0.24 (0.29–0.29)	.522
Membranous septum length (mm)	6.2 ± 1.1	6.3 ± 1.0	5.4 ± 0.9	<.001	6.4 ± 1.0	5.6 ± 1.1	.001
MAC Agatston score	271 (0–1478)	257 (0–1686)	314 (135–645)	.264	282 (0–1699)	234 (16–645)	.215
MAC volume (mm^3)	223 (0–1152)	208 (0–1403)	274 (113–505)	.292	285 (0–1454)	212 (13–505)	.243
Presence of AMCC	72 (45.0)	57 (41.0)	15 (71.4)	.009	52 (39.4)	20 (71.4)	.002
AMCC proximity type				.040			.007
RFT-dominant	26 (36.1)	19 (73.1)	7 (26.9)		17 (65.4)	9 (34.6)	
LFT-dominant	14 (19.4)	12 (85.7)	2 (14.3)		12 (85.7)	2 (14.3)	
Bilateral	32 (44.4)	26 (81.3)	6 (18.8)		23 (71.9)	9 (28.1)	
AMCC Agatston score	0 (0–180)	0 (0–142)	182 (0–292)	.038	0 (0–118)	172 (2–302)	.009
AMCC volume (mm^3)	0 (0–146)	0 (0–117)	146 (4–235)	.045	0 (0–96)	131 (2–249)	.010
AVC Agatston score	2167 (1457–3280)	2157 (1365–3280)	2488 (2016–3274)	.162	2153 (1345–3265)	2433 (2006–3400)	.125
AVC volume (mm^3)	1761 (1191–2688)	1753 (1141–2688)	2050 (1617–2741)	.169	1751 (1121–2687)	2034 (1597–2885)	.115

Note: Values represent mean ± SD, *n* (%), or median (interquartile range).

Abbreviations: AMCC, aorto-mitral continuity calcification; AV, atrioventricular; AVC, aortic valve calcification; CT, computed tomography; LFT, left fibrous trigone MAC, mitral annular calcification; PPM, permanent pacemaker; OR, odds ratio; RFT, right fibrous trigone.

PPM implantation (OR, 5.39; CI, 1.75–16.55; $p = .002$). The presence of AMCC alone conferred respective increases in risk of 4.20- and 4.44-fold (OR: 4.20, 95% CI: 1.19–14.87, $p = .026$ for HAVB; OR: 4.44, 95% CI: 1.56–12.60, $p = .004$ for PPM).

The most striking results were observed in Model 3, which categorized AMCC by proximity type. In this model, RFT-dominant AMCC was a strong independent predictor, associated with a 9.22-fold increase in the risk of HAVB (OR, 9.22; 95% CI, 1.63–51.99; $p = .012$) and a 7.62-fold increase in the risk of PPM (OR, 7.62; 95% CI, 1.91–30.38; $p = .004$). Bilateral AMCC also significantly increased the risk (OR, 7.46; 95% CI, 1.39–39.85; $p = .019$ for HAVB and OR, 7.07; 95% CI, 1.86–26.77; $p = .005$ for PPM). These findings underscore the importance of not only the quantity but also the anatomical location of AMCC. Across all models, QRS duration, MS length, and ID were robust and consistent predictors of CD.

4 | DISCUSSION

This study provides new insights into the relationship between AMCC and CD in patients undergoing TAVI with the Myval THV. To our knowledge, this is the first study to evaluate this relationship using the Myval valve and incorporate AMCC distribution into risk assessment. The key findings are as follows: (1) An AMCC score > 180 independently predicted HAVB (5.58-fold) and PPM (5.39-fold); (2) AMCC distribution, particularly proximity to the RFT, was associated with a higher risk of CD, highlighting the anatomical relevance of calcification location. (III) Greater ID, shorter MS length, and prolonged QRS duration were also independent predictors of CD. These results highlight AMCC as a powerful anatomical risk factor and support the integration of both the extent and location of calcification into pre-TAVI evaluations.

4.1 | Mechanisms linking AMCC to CD

The AMC constitutes a fibrous structure extending from the LFT at the posterior left coronary leaflet to the RFT between the right and noncoronary leaflets. It plays a crucial role in maintaining the structural integrity of the left heart.[5,6] Anatomically, the AMC is closely associated with the central fibrous body, forming a structural bridge between the LFT and the left ventricular myocardium, and connecting to the MS via the RFT. The AV node is in direct contact with the central fibrous body and gives rise to the bundle of His, which traverses the fibrous body on the left side before penetrating the MS. Given the proximity of the conduction system to the AMC, radial forces applied to the AMC in the presence of extensive calcification may result in conduction abnormalities, such as HAVB requiring PPM. The relationship between AMCC and CD can be explained by two primary mechanisms. First, AMCC may exacerbate mechanical

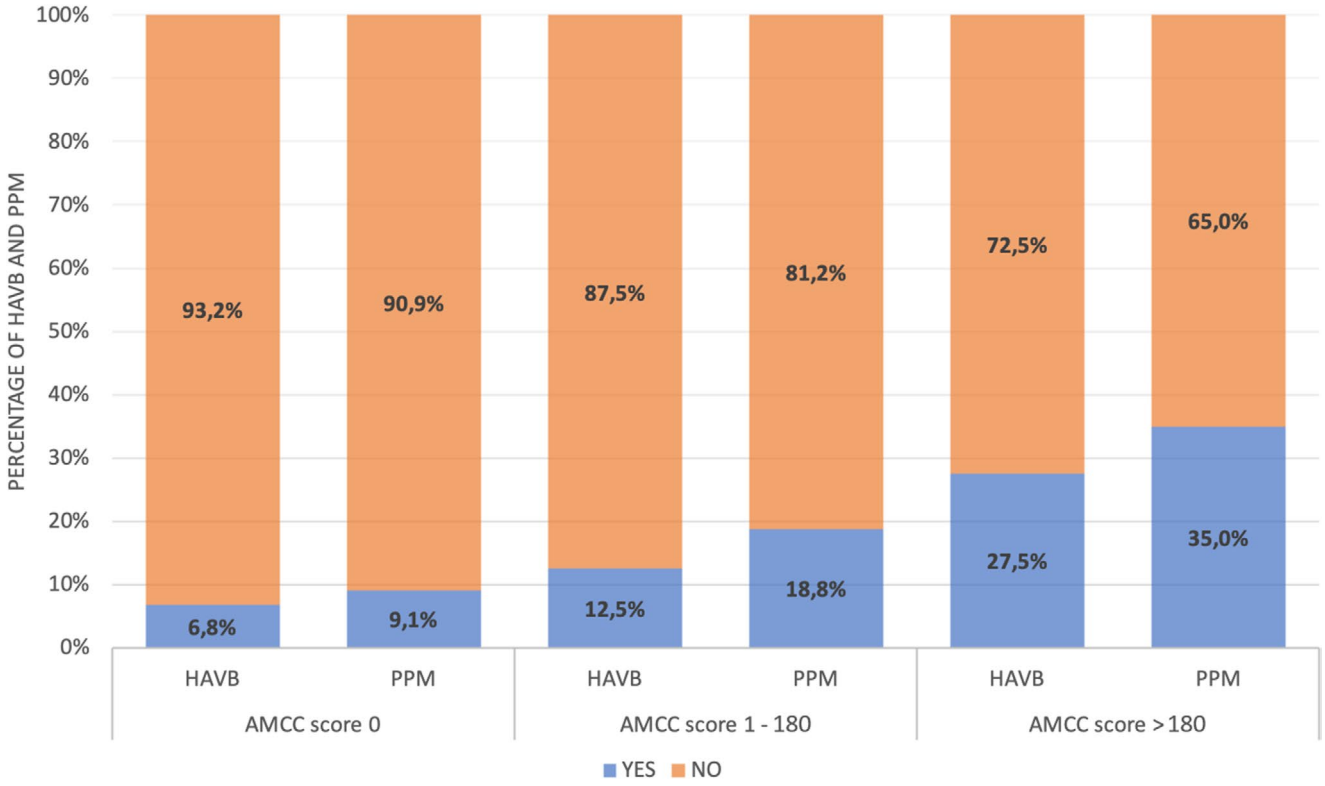

FIGURE 2 Incidence of high-degree atrioventricular block (HAVB) and permanent pacemaker (PPM) implantation according to the severity of aortomitral continuity calcification (AMCC).

stress on the AV node and its fibers during valve deployment, increasing susceptibility to conduction injury. Second, AMCC may reflect pre-existing degeneration of the conduction system, making it more vulnerable to procedural trauma. Consistent with these pathophysiological mechanisms, the present study demonstrated that AMCC was significantly associated with HAVB and PPM, with affected patients showing higher prevalence, scores, and volumes of AMCC. Notably, stratifying patients by AMCC score revealed a stepwise increase in the risk of developing CD, supporting its value as a predictive tool in preprocedural assessment.

4.2 | Comparison with previous studies

Previous studies have investigated the relationship between extensive aortic valve and root calcification and conduction abnormalities, including the need for PPM following TAVI.[17–20] However, these studies have often focused on the calcification of the aortic valve leaflets themselves. The present study expands on this knowledge by highlighting the role of AMCC as an independent predictor of CD, which might not have been fully appreciated in earlier studies. The prevalence of AMCC in this study (45.0%) aligns with prior research reporting a range of 41.9%–48.9% among TAVI candidates.[8,9] Previous research has demonstrated a consistent association between AMCC and CD after TAVI. For instance, Katchi et al. observed that patients requiring PPM had a higher prevalence of AMCC (69% vs. 32%; $p < .0001$) and significantly higher AMCC scores compared to those without PPM. They also reported that AMCC scores greater than 300 were associated with a fivefold increased OR for PPMI (OR, 5.7; $p = .0016$).[8] Despite the robust findings of these studies, they were limited by heterogeneity in valve types and generations and variable procedural techniques. Additionally, MS length and ID are now regarded as significant risk factors and independent predictors of damage to the AV conduction axis.[21,22] In the aforementioned study, the multivariate analysis did not include MS or ID, which may have affected the results. Finally, endpoints often focused on PPM rather than comprehensive CD outcomes, limiting their scope.

This study is distinguished by several novel contributions, most notably its detailed evaluation of AMCC distribution—a factor not previously incorporated into multivariate analyses in earlier research. By categorizing the anatomical proximity of AMCC to the LFT and RFT, this study introduces a novel approach to understanding how the specific localization of calcification may influence the risk of CD. Notably, AMCC involvement near the RFT—an area adjacent to the penetrating His bundle—was found to confer a higher risk of HAVB and PPM. This distributional analysis provides a more refined anatomical risk assessment than the total AMCC burden alone. It also underscores the importance of quantifying and anatomically localizing calcification in preprocedural evaluations.

In contrast to previous studies that primarily evaluated the impact of AMCC with early-generation valves, all patients in our cohort were treated exclusively with the newer-generation Myval THV. More recently, the LANDMARK trial provided high-level evidence

TABLE 3 Procedural characteristics.

	All patients (*N* = 160)	High-degree AV block		*p*-Value	PPM implantation		*p*-Value
		No (*N* = 139)	Yes (*N* = 21)		No (*N* = 132)	Yes (*N* = 28)	
Procedural characteristics							
Conscious sedation	133 (83.1)	118 (84.9)	15 (71.4)	.129	112 (84.8)	21 (75.0)	.264
Procedure time,[a] min	83.1 ± 29.4	82.6 ± 28.6	86.0 ± 34.9	.627	82.4 ± 27.7	86.1 ± 36.5	.551
Total contrast used (mL)	150 (107–200)	150 (100–200)	155 (135–230)	.379	150 (100–200)	180 (130–230)	.238
ICU stay, days	2.0 (1.0–4.0)	2.0 (1.0–4.0)	4.0 (3.0–7.0)	.037	2.0 (1.0–4.0)	4.0 (3.0–7.0)	.021
Discharge time, days	9.0 (5.0–15.0)	9.0 (5.0–13.5)	13.0 (7.0–23.5)	.026	8.0 (5.0–13.0)	13.0 (8.2–24.7)	.006
Valve size, mm	27.5 (24.5–29)	26.0 (24.5–27.5)	29.0 (25.2–29.0)	.038	26.0 (24.5–27.5)	28.2 (24.5–29.0)	.074
Predilatation	60 (37.5)	48 (34.5)	12 (57.1)	.046	45 (34.1)	15 (53.6)	.053
Postdilatation	62 (38.8)	53 (38.1)	9 (42.9)	.679	49 (37.1)	13 (46.4)	.359
Pre- and postdilatation	26 (16.3)	21 (15.1)	5 (23.8)	.342	19 (14.4)	7 (25.0)	.169
Implantation depth (mm)	6.6 ± 2.0	6.4 ± 2.0	8.0 ± 1.4	.002	6.4 ± 2.0	7.8 ± 1.5	.001
Postprocedural aortic valve mean gradient (mmHg)	7.6 ± 4.0	7.6 ± 3.7	7.6 ± 5.8	.967	7.6 ± 3.7	7.5 ± 5.1	.825

Note: Values represent mean ± SD, *n* (%), or median (interquartile range).

Abbreviations: AV, atrioventricular; ICU, intensive care unit; PPM, permanent pacemaker.

[a]Procedure time was defined as the time from arterial puncture until vascular closure.

to support the use of the Myval valve series in patients indicated for TAVI.[23] This randomized controlled trial demonstrated noninferiority of the Myval valve compared to FDA-approved, commercially available valves (either the SAPIEN THV or Evolut THV series) in terms of clinical outcomes (one-sided upper 95% CI 3.8, $p < .0001$ [noninferiority]). This ensures that the observed results are attributable to AMCC and eliminates confounding related to device heterogeneity seen in prior studies, which included multiple valve platforms of different generations.

In the present study, we have included key anatomical and procedural predictors, such as MS length and ID, which were not analyzed in the multivariable models of prior AMCC studies. Our findings underscore the importance of ID as a modifiable procedural factor influencing the risk of post-TAVI CD. A significantly greater ID was observed in patients who developed HAVB and required PPM. This finding suggests that deeper valve positioning may result in increased mechanical stress on the AV conduction axis, particularly in patients with shorter MS lengths where the conduction tissue is in close proximity to the device. Given these findings, it may be advisable to avoid deep implantation of the Myval valve to minimize the risk of conduction damage. Tailoring the ID, especially in patients identified pre-procedurally as having a short MS length or a high AMCC burden, could be a critical step in reducing postprocedural CD and the subsequent need for PPM. Unlike previous studies that have focused primarily on the need for PPM, we analyzed a composite endpoint of CD (HAVB and PPM), providing a broader and more clinically meaningful assessment of CD after TAVI. Another important finding of our study is that prolonged QRS duration was independently associated with an increased risk of HAVB and PPM. This finding supports prior evidence that baseline QRS widening may reflect underlying conduction system vulnerability, increasing susceptibility to procedural injury.[24,25]

4.3 | Future directions

Future research should focus on a more granular analysis of the relationship between AMCC and specific types of CD. The precise anatomical location and degree of calcification in relation to the conduction system could provide valuable insights into the pathophysiological mechanisms underlying these disturbances. The role of preoperative imaging in predicting CD should also be further explored. Advanced imaging techniques such as high-resolution CT scans or cardiac magnetic resonance imaging may allow for better preoperative assessment of AMCC and its potential impact on conduction pathways. Integration of these imaging modalities into routine pre-TAVI evaluation could help improve risk stratification and guide decision making.

4.4 | Limitations of the study

While our study demonstrates a strong association between AMCC and CD, it is important to acknowledge certain limitations. First, this

TABLE 4 Predictors of HAVB.

Variable	OR (95% CI)	*p*-Value
Univariable analysis		
Age	1.04 (0.97–1.13)	.226
Sex (male)	1.36 (0.54–3.42)	.506
Preoperative PR interval	1.00 (0.99–1.01)	.650
Preoperative QRS duration	1.04 (1.01–1.06)	.001
Atrial fibrillation	0.62 (0.19–1.97)	.424
Membranous septum length	0.37 (0.21–0.65)	<.001
MAC score	1.0 (0.99–1.0)	.233
AVC score	1.0 (1.0–1.0)	.168
Presence of AMCC[a]	3.59 (1.31–9.82)	.013
AMCC proximity type		.059
No AMCC	1.0 (reference)	
RFT-dominant	5.03 (1.51–16.70)	.008
LFT-dominant	2.27 (0.41–12.60)	.346
Bilateral	3.15 (0.93–10.62)	.064
AMCC score, categorical		.010
AMCC score 0	1.0 (reference)	
AMCC score 1–180	1.95 (0.51–7.42)	.326
AMCC score > 180	5.18 (1.75–15.28)	.003
Annulus eccentricity	0.57 (0.42–7.97)	.681
Valve size	1.20 (1.00–1.43)	.042
Balloon predilatation	2.52 (0.99–6.42)	.051
Balloon postdilatation	1.21 (0.48–3.08)	.679
Implantation depth	1.51 (1.15–1.99)	.003

	Model 1 for categorical AMCC		Model 2 for binary AMCC		Model 3 for AMCC proximity[b]	
Variable	OR (95% CI)	*p*-Value	OR (95% CI)	*p*-Value	OR (95% CI)	*p*-Value
Multivariable analysis						
Preoperative QRS duration	1.03 (1.00–1.06)	.010	1.03 (1.00–1.06)	.009	1.04 (1.01–1.07)	.004
Membranous septum length	0.43 (0.22–0.81)	.009	0.43 (0.23–0.81)	.008	0.35 (0.17–0.72)	.004
Valve size	1.13 (0.92–1.38)	.231	1.13 (0.94–1.39)	.212	1.15 (0.92–1.48)	.186
Balloon predilatation	1.42 (0.46–4.42)	.538	1.39 (0.45–4.30)	.561	1.44 (0.46–4.44)	.516
Implantation depth	1.64 (1.13–2.38)	.009	1.62 (1.13–2.34)	.010	1.73 (1.16–2.58)	.007
AMCC Score, categorical		.045				
AMCC score 0	1.0 (reference)					
AMCC score 1–180	2.37 (0.45–12.43)	.306				
AMCC score > 180	5.58 (1.43–21.70)	.013				
Presence of AMCC[a]			4.20 (1.19–14.87)	.026		
AMCC proximity type						.014
No AMCC					1.0 (reference)	
RFT-dominant					9.22 (1.63–51.99)	.012
LFT-dominant					0.48 (0.05–4.46)	.522
Bilateral					7.46 (1.39–39.85)	.019

Abbreviations: AMCC, aortomitral continuity calcification; AVC, aortic valve calcification; CI, confidence interval; LFT, left fibrous trigone; MAC, mitral annular calcification; OR, odds ratio; RFT, right fibrous trigone.

[a]Presence of AMCC was analyzed as a binary variable.

[b]Model 3 includes AMCC localization categorized by proximity to the left fibrous trigone, right fibrous trigone, or both.

TABLE 5 Predictors of PPM implantation.

Variable	OR (95% CI)	*p*-Value
Univariable analysis		
Age	1.0 (0.97–1.10)	.286
Sex (male)	1.47 (0.64–3.33)	.354
Preoperative PR interval	1.0 (0.99–1.01)	.464
Preoperative QRS duration	1.03 (1.01–1.05)	.003
Atrial fibrillation	0.55 (0.19–1.57)	.271
Membranous septum length	0.50 (0.32–0.78)	.002
MAC score	1.0 (0.99–1.0)	.192
AVC score	1.0 (1.0–1.0)	.131
Presence of AMCC[a]	3.84 (1.57–9.37)	.003
AMCC proximity type		.012
No AMCC	1.0 (reference)	
RFT-dominant	5.29 (1.78–15.69)	.003
LFT-dominant	1.66 (0.31–8.80)	.547
Bilateral	3.91 (1.35–11.28)	.012
AMCC Score, categorical		.003
AMCC score 0	1.0 (reference)	
AMCC score 1–180	2.30 (0.73–7.26)	.153
AMCC score > 180	5.38 (2.03–14.27)	.001
Annulus eccentricity	0.49 (0.02–11.06)	.655
Valve size	1.14 (0.98–1.33)	.077
Balloon predilatation	2.23 (0.97–5.09)	.057
Balloon postdilatation	1.46 (0.64–3.34)	.360
Implantation depth	1.44 (1.13–1.82)	.002

	Model 1 for categorical AMCC		Model 2 for binary AMCC		Model 3 for AMCC proximity[b]	
Variable	**OR (95% CI)**	***p*-Value**	**OR (95% CI)**	***p*-Value**	**OR (95% CI)**	***p*-Value**
Multivariable analysis						
Preoperative QRS duration	1.02 (0.99–1.05)	.037	1.02 (1.00–1.05)	.033	1.03 (1.00–1.06)	.013
Membranous septum length	0.58 (0.35–0.97)	.042	0.59 (0.35–0.98)	.041	0.52 (0.30–0.94)	.018
Valve size	1.09 (0.91–1.29)	.304	1.09 (0.92–1.30)	.281	1.12 (0.92–1.34)	.242
Balloon predilatation	1.12 (0.41–2.98)	.808	1.13 (0.42–2.98)	.803	1.16 (0.40–2.99)	.783
Implantation depth	1.51 (1.13–2.02)	.005	1.52 (1.13–2.02)	.004	1.52 (1.13–2.02)	.004
AMCC Score, categorical		.013				
AMCC score 0	1.0 (reference)					
AMCC score 1–180	3.06 (0.80–11.69)	.101				
AMCC score > 180	5.39 (1.75–16.55)	.002				
Presence of AMCC[a]			4.44 (1.56–12.60)	.004		
AMCC proximity type						.002
No AMCC					1.0 (reference)	
RFT-dominant					7.62 (1.91–30.38)	.004
LFT-dominant					0.46 (0.06–3.42)	.450
Bilateral					7.07 (1.86–26.77)	.005

Abbreviations: AMCC, aortomitral continuity calcification; AVC, aortic valve calcification; CI, confidence interval; LFT, left fibrous trigone; MAC, mitral annular calcification; OR, odds ratio; RFT, right fibrous trigone.

[a]Presence of AMCC was analyzed as a binary variable.

[b]Model 3 includes AMCC localization categorized by proximity to the left fibrous trigone, right fibrous trigone, or both.

single-center retrospective analysis is limited by its relatively small sample size. The sample size, although sufficient to detect significant associations, may limit the generalizability of our findings to broader patient populations. Additionally, the number of patients with RBBB in our study was small, which limited our ability to include RBBB in the multivariable regression analysis. As a result, potential associations between RBBB and CD could not be fully evaluated. Future multicenter, prospective studies with larger cohorts are needed to validate our results and further elucidate the underlying mechanisms. Second, the impact of AMCC on long-term outcomes, such as survival and quality of life, was not assessed in this study. Further research should aim to evaluate whether AMCC as a predictor of CD translates into clinically significant differences in these long-term outcomes, particularly in high-risk patients who may require more intensive post-TAVI management. Finally, there may be some subjectivity in our AMCC scoring method, especially when faced with the adjacent structure of annular and subannular calcification; both intra- and inter-observer reproducibility of CT measurements were good.

5 | CONCLUSION

This study establishes the significance of AMCC as a key predictor of CD following TAVI with the Myval THV. Higher AMCC scores, particularly those exceeding 180, were independently associated with a heightened risk of new-onset CD, including HAVB and PPM implantation. Importantly, not only the burden but also the anatomical distribution of AMCC influenced risk, with RFT-dominant calcification emerging as a significant predictor. Shorter MS length and greater ID were also independently associated with CD. These findings support the routine preprocedural assessment of both AMCC burden and proximity type to improve risk stratification and optimize procedural planning in TAVI patients.

ACKNOWLEDGMENTS

None.

FUNDING INFORMATION

None.

CONFLICT OF INTEREST STATEMENT

The authors declare no conflict of interest for this article.

DATA AVAILABILITY STATEMENT

Data are available upon request to the corresponding author.

ETHICS STATEMENT

This retrospective study was conducted at the University of Health Sciences Istanbul Mehmet Akif Ersoy Thoracic and Cardiovascular Surgery Training and Research Hospital after approval by the hospital's Institutional Review Board (Date of IRB approval: 19.11.2024, IRB approval number: 2024.06-64).

INFORMED CONSENT

Informed consent was obtained from all subjects involved in the study.

ORCID

Serkan Aslan https://orcid.org/0000-0001-9112-5754
Aysel Türkvatan https://orcid.org/0000-0002-3150-5787
Mehmet Kanyılmaz https://orcid.org/0009-0002-2500-1029
Burçin Yılmaz https://orcid.org/0009-0004-5586-2756
Dilara Pay https://orcid.org/0000-0001-9434-432X
Kadir Sadıkoğlu https://orcid.org/0009-0004-3532-378X
Hande Uysal https://orcid.org/0009-0000-0543-7904
Gökhan Demirci https://orcid.org/0000-0003-2835-7530
Mehmet Altunova https://orcid.org/0000-0001-5351-5022
Serkan Kahraman https://orcid.org/0000-0003-2796-0987
Mehmet Ertürk https://orcid.org/0000-0002-2468-2793

REFERENCES

1. Reardon MJ, Van Mieghem NM, Popma JJ, Kleiman NS, Søndergaard L, Mumtaz M, et al. Surgical or transcatheter aortic-valve replacement in intermediate-risk patients. N Engl J Med. 2017;376(14):1321–31. https://doi.org/10.1056/NEJMoa1700456
2. Sardar P, Kundu A, Chatterjee S, Feldman DN, Owan T, Kakouros N, et al. Transcatheter versus surgical aortic valve replacement in intermediate-risk patients: evidence from a meta-analysis. Catheter Cardiovasc Interv. 2017;90(3):504–15. https://doi.org/10.1002/ccd.27041
3. Mangieri A, Montalto C, Pagnesi M, Lanzillo G, Demir O, Testa L, et al. TAVI and Post procedural cardiac conduction abnormalities. Front Cardiovasc Med. 2018;5:85. https://doi.org/10.3389/fcvm.2018.00085
4. Halapas A, Koliastasis L, Doundoulakis I, Antoniou CK, Stefanadis C, Tsiachris D. Transcatheter aortic valve implantation and conduction disturbances: focus on clinical implications. J Cardiovasc Dev Dis. 2023;10(11):469. https://doi.org/10.3390/jcdd10110469
5. Saremi F, Sánchez-Quintana D, Mori S, Muresian H, Spicer DE, Hassani C, et al. Fibrous skeleton of the heart: anatomic overview and evaluation of pathologic conditions with CT and MR imaging. Radiographics. 2017;37(5):1330–51. https://doi.org/10.1148/rg.2017170004
6. Mori S, Fukuzawa K, Takaya T, Takamine S, Ito T, Fujiwara S, et al. Clinical cardiac structural anatomy reconstructed within the cardiac contour using multidetector-row computed tomography: left ventricular outflow tract. Clin Anat. 2016;29(3):353–63. https://doi.org/10.1002/ca.22547
7. Aslan S, Türkvatan A, Topel Ç, Güner A, Demir AR, Kahraman S, et al. Structural changes of the right fibrous trigone as a risk factor for conduction disturbance after transcatheter aortic valve implantation. Anatol J Cardiol. 2022;26(7):532–42. https://doi.org/10.5152/AnatolJCardiol.2022.987
8. Katchi F, Bhatt D, Markowitz SM, Szymonifka J, Cheng EP, Minutello RM, et al. Impact of aortomitral continuity calcification on need for permanent pacemaker after transcatheter aortic valve replacement. Circ Cardiovasc Imaging. 2019;12(12):e009570. https://doi.org/10.1161/CIRCIMAGING.119.009570
9. Ryś M, Hryniewiecki T, Witkowski A, Michałowska I, Zatorska K, Stokłosa P, et al. Association between calcifications of mitro-aortic continuity and mitral regurgitation in patients undergoing transcatheter aortic valve replacement. Kardiol Pol. 2021;79(6):669–75. https://doi.org/10.33963/KP.15987

10. Willemink MJ, Maret E, Moneghetti KJ, Kim JB, Haddad F, Kobayashi Y, et al. Incremental value of aortomitral continuity calcification for risk assessment after transcatheter aortic valve replacement. Radiol Cardiothorac Imaging. 2019;1(5):e190067. https://doi.org/10.1148/ryct.2019190067
11. Agatston AS, Janowitz WR, Hildner FJ, Zusmer NR, Viamonte M Jr, Detrano R. Quantification of coronary artery calcium using ultrafast computed tomography. J Am Coll Cardiol. 1990;15(4):827–32. https://doi.org/10.1016/0735-1097(90)90282-t
12. Hamdan A, Guetta V, Klempfner R, Konen E, Raanani E, Glikson M, et al. Inverse relationship between membranous septal length and the risk of atrioventricular block in patients undergoing transcatheter aortic valve implantation. JACC Cardiovasc Interv. 2015;8(9):1218–28. https://doi.org/10.1016/j.jcin.2015.05.010
13. Aslan S, Demir AR, Çelik Ö, Kalkan AK, Uzun F, Güner A, et al. Usefulness of membranous septum length in the prediction of major conduction disturbances in patients undergoing transcatheter aortic valve replacement with different devices. Kardiol Pol. 2020;78(10):1020–8. https://doi.org/10.33963/KP.15538
14. Généreux P, Piazza N, Alu MC, Nazif T, Hahn RT, Pibarot P, et al. Valve academic research consortium 3: updated endpoint definitions for aortic valve clinical research. J Am Coll Cardiol. 2021;77(21):2717–46. https://doi.org/10.1016/j.jacc.2021.02.038
15. Surawicz B, Childers R, Deal BJ, Gettes LS, Bailey JJ, Gorgels A, et al. AHA/ACCF/HRS recommendations for the standardization and interpretation of the electrocardiogram: part III: intraventricular conduction disturbances: a scientific statement from the American Heart Association electrocardiography and arrhythmias committee, council on clinical cardiology; the American College of Cardiology Foundation; and the Heart Rhythm Society. Endorsed by the International Society for Computerized Electrocardiology. J Am Coll Cardiol. 2009;53(11):976–81. https://doi.org/10.1016/j.jacc.2008.12.013
16. Glikson M, Nielsen JC, Kronborg MB, Michowitz Y, Auricchio A, Barbash IM, et al. 2021 ESC guidelines on cardiac pacing and cardiac resynchronization therapy. Eur Heart J. 2021;42(35):3427–520. https://doi.org/10.1093/eurheartj/ehab364
17. Pollari F, Großmann I, Vogt F, Kalisnik JM, Cuomo M, Schwab J, et al. Risk factors for atrioventricular block after transcatheter aortic valve implantation: a single-centre analysis including assessment of aortic calcifications and follow-up. Europace. 2019;21(5):787–95. https://doi.org/10.1093/europace/euy316
18. Fujita B, Kütting M, Seiffert M, Scholtz S, Egron S, Prashovikj E, et al. Calcium distribution patterns of the aortic valve as a risk factor for the need of permanent pacemaker implantation after transcatheter aortic valve implantation. Eur Heart J Cardiovasc Imaging. 2016;17(12):1385–93. https://doi.org/10.1093/ehjci/jev343
19. Guimarães L, Ferreira-Neto AN, Urena M, Nombela-Franco L, Wintzer-Wehekind J, Levesque MH, et al. Transcatheter aortic valve replacement with the balloon-expandable SAPIEN 3 valve: impact of calcium score on valve performance and clinical outcomes. Int J Cardiol. 2020;306:20–4. https://doi.org/10.1016/j.ijcard.2020.02.047
20. Mauri V, Reimann A, Stern D, Scherner M, Kuhn E, Rudolph V, et al. Predictors of permanent pacemaker implantation after transcatheter aortic valve replacement with the SAPIEN 3. JACC Cardiovasc Interv. 2016;9(21):2200–9. https://doi.org/10.1016/j.jcin.2016.08.034
21. Siontis GC, Jüni P, Pilgrim T, Stortecky S, Büllesfeld L, Meier B, et al. Predictors of permanent pacemaker implantation in patients with severe aortic stenosis undergoing TAVR: a meta-analysis. J Am Coll Cardiol. 2014;64(2):129–40. https://doi.org/10.1016/j.jacc.2014.04.033
22. Sá MP, Van den Eynde J, Jacquemyn X, Erten O, Rodriguez R, Goldman S, et al. Computed tomography-derived membranous septum length as predictor of conduction abnormalities and permanent pacemaker implantation after TAVI: a meta-analysis of observational studies. Catheter Cardiovasc Interv. 2023;101(7):1203–13. https://doi.org/10.1002/ccd.30666
23. Baumbach A, van Royen N, Amat-Santos IJ, Hudec M, Bunc M, Ijsselmuiden A, et al. LANDMARK comparison of early outcomes of newer-generation Myval transcatheter heart valve series with contemporary valves (Sapien and Evolut) in real-world individuals with severe symptomatic native aortic stenosis: a randomised non-inferiority trial. Lancet. 2024;403(10445):2695–708. https://doi.org/10.1016/S0140-6736(24)00821-3
24. Sharma E, Chu AF. Predictors of right ventricular pacing and pacemaker dependence in transcatheter aortic valve replacement patients. J Interv Card Electrophysiol. 2018;51(1):77–86. https://doi.org/10.1007/s10840-017-0303-1
25. Nwaedozie S, Zhang H, Najjar Mojarrab J, Sharma P, Yeung P, Umukoro P, et al. Novel predictors of permanent pacemaker implantation following transcatheter aortic valve replacement. World J Cardiol. 2023;15(11):582–98. https://doi.org/10.4330/wjc.v15.i11.582

How to cite this article: Aslan S, Türkvatan A, Kanyılmaz M, Yılmaz B, Pay D, Sadıkoğlu K, et al. Association between aortomitral continuity calcification and conduction disturbances following transcatheter aortic valve implantation with the balloon-expandable Myval valve. J Arrhythmia. 2025;41:e70140. https://doi.org/10.1002/joa3.70140